ELSEVIER

14 December 1998

PHYSICS LETTERS A

Physics Letters A 249 (1998) 483–488

Bloch particle in the presence of dc and ac fields

M. Glück [a], A.R. Kolovsky [a,b,1], H.J. Korsch [a]

[a] *Fachbereich Physik, Universität Kaiserslautern, D-67653 Kaiserslautern, Germany*
[b] *L.V. Kirensky Institute of Physics, 660036 Krasnoyarsk, Russia*

Received 22 May 1998; revised manuscript received 18 September 1998; accepted for publication 20 September 1998
Communicated by L.J. Sham

Abstract

In this Letter we study the metastable states of a Bloch particle in the presence of external ac and dc fields. For the resonance condition between the period of the driving frequency and the Bloch period, the complex quasi-energies are numerically calculated for two qualitatively different regimes (quasi-regular and chaotic) of the system dynamics. For the chaotic regime an effect of quantum stabilization, which suppresses the classical decay mechanism, is found. This effect is demonstrated to be a kind of quantum phenomenon sensitive to the resonance condition. © 1998 Elsevier Science B.V.

PACS: 73.20.Dx; 73.40.Gk; 05.45.+b
Keywords: Wannier–Bloch states; Quantum chaos

In this Letter we study quantum states of a Bloch particle in the presence of external dc and ac fields,

$$H = p^2/2 + \cos x + Fx + F_\omega x \sin(\omega t)\,. \qquad (1)$$

The system (1) has been discussed in the context of solid state physics for at least 50 years, but is still of some recent interest [2]. The main bulk of results so far known concerns the case of a static field $F_\omega = 0$ (see, for example, the reviews [2,3]) or a pure oscillatory field $F = 0$ [4–6]. In the general case, $F \neq 0$, $F_\omega \neq 0$, our knowledge about the system is rather poor and mainly based on studies of the tight-binding model [7–9]. However, the use of the tight-binding model, which most frequently amounts to using a one-band approximation, can leave aside a number of phenomena. For example, neglecting interband transitions in the case of a pure dc field transforms the Wannier–Stark resonances (metastable states [3]) into stationary, exponentially localized eigenfunctions. In the pure oscillatory case, using a one-band approximation reduces the phase space of the generally chaotic system (1) to a cylinder and, thus, eliminates the phenomenon of chaotic diffusion of the momentum. In this present paper we study the system states *beyond* the one-band approximation. From the preliminary remarks above these states are expected to be a kind of "chaotic"

[1] E-mail: kolovsky@physik.uni-kl.de.

[2] We also mention that recently the subject received new impetus from experiments with neutral atoms in an optical lattice, which suggest an almost perfect realization of a one-dimensional Hamiltonian (1), see Ref. [1]

[3] To avoid a misunderstanding, we note from the very beginning that the term "resonance" is used in this paper in three different contexts. First, we use "resonance" as a synonym of the "metastable state" [2]; second, this term is used to identify the classical nonlinear resonance [12] and its quantum counterpart; third it is used to distinguish the resonance condition between the Bloch period and the period of the driving frequency [16].

PII S0375-9601(98)00763-4

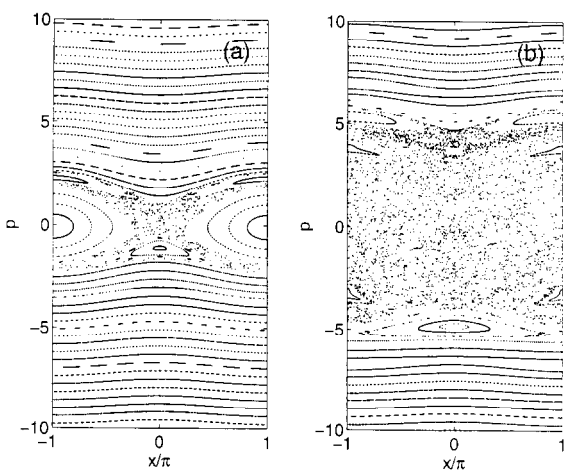

Fig. 1. Phase portrait of the system (2) for $F = 0$. Coordinates $x(t_n)$ and momentum $p(t_n)$ of a classical particle for times t_n being the multiple of the driving frequency period are plotted for 50 different initial conditions. The driving frequency $\omega = 10/6$, scaled driving amplitude $\epsilon = 0.1$ (a), and $\epsilon = 1.5$ (b).

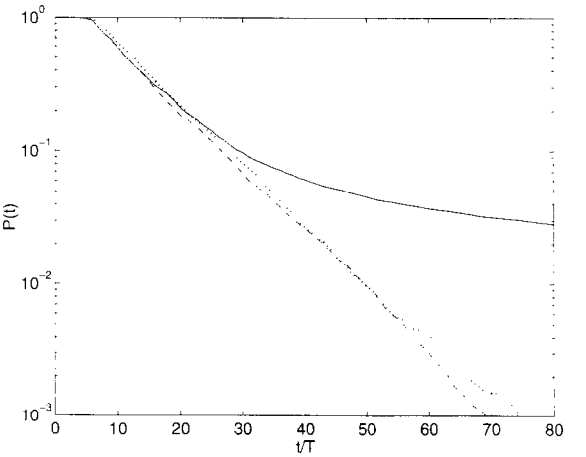

Fig. 2. Comparison between classical and quantum decay processes for $F = \omega/4\pi \approx 0.13$ in the chaotic case (b). The dotted line shows the classical decay, the solid line is the quantum decay for the resonance condition $T_\omega = T_B$ ($\hbar = 1/2$), and the dashed line is the slightly off resonance case ($\hbar = 0.5109531$).

metastable states [11].

We begin with the classical analysis. It is convenient to include the ac term in the Hamiltonian (1) in the periodic potential, which is done by the usual gauge transformation $p \to p + (F_\omega/\omega)\cos(\omega t)$, $x \to x + (F_\omega/\omega^2)\sin(\omega t)$. Then the Hamiltonian (1) takes the form

$$H = \frac{p^2}{2} + \cos[x - \epsilon\sin(\omega t)] + Fx\,, \quad \epsilon = \frac{F_\omega}{\omega^2}\,. \quad (2)$$

It is also useful to expand the "new" time-dependent potential in the Fourier series

$$\cos[x - \epsilon\sin(\omega t)] = J_0(\epsilon)\cos x + \sum_{m=1}^{\infty} J_m(\epsilon) \times [\cos(x - m\omega t) + (-1)^m \cos(x + m\omega t)]\,. \quad (3)$$

It follows from Eqs. (2), (3), that for $F = 0$ the system (1) is a system of many interacting nonlinear resonances and, therefore, its dynamics can be either quasi-regular or chaotic depending on a particular choice of the parameters ω and ϵ [12]. Here we restrict ourselves to the choice (a) $\omega = 10/6$, $\epsilon = 0.1$, where the system dynamics is almost regular, and (b) $\omega = 10/6$, $\epsilon = 1.5$, where a developed chaos exists. Fig. 1 shows phase portraits of the system for these two cases. For small ϵ only three terms in Eq. (3), $J_0(\epsilon)\cos x$ and $J_{\pm 1}\cos(x \pm \omega t)$, are important [13] – three nonlinear resonances originated by these terms are well seen in Fig. 1a. For large ϵ many such resonances overlap and chaotic diffusion is possible. We note, however, that the classical motion always remains bounded in momentum space for $F = 0$.

Adding a weak dc field cardinally changes the system dynamics. The static field destroys the invariant curves separating the chaotic component from the outer region of regular motion. Thus, the chaotic component can not support a bounded (in momentum space) motion for an infinite time. However, it can support a bounded motion temporally. The dotted line in Fig. 2 shows the probability $P_{\rm cl}(t)$ of a classical particle to stay within the chaotic region for the parameters of Fig. 1b and $F \approx 0.13$. (The classical probability was calculated by simulating the dynamics of $N = 40\,000$ particles with initial conditions around $x = 0, p = 0$. Then the function $P_{\rm cl}(t)$ denotes the relative number of the particles with momentum $|p| < 6$.) It is seen that the probability decays exponentially with a classical decay time $\tau_{\rm cl} \approx 10T_\omega$. This transient chaotic (actually diffusive) dynamics of the system is in contrast with the accelerated motion observed in the outer region of negative momentum (we fix $F > 0$, so that a particle is accelerated towards minus infinity). It should also be noted that the homogeneous static field not necessarily destroys the invariant curves separating the chaotic component from

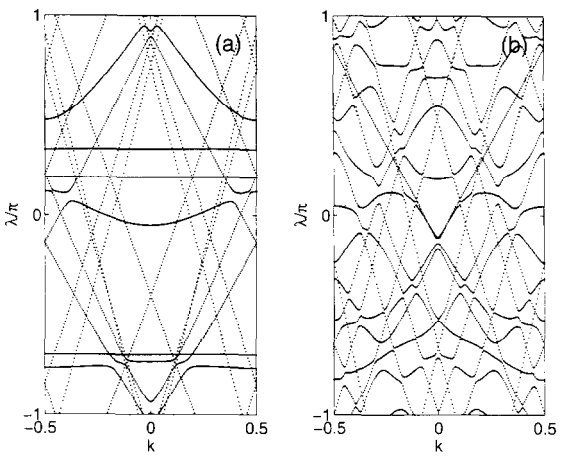

Fig. 3. Quasi-energy spectrum $\lambda = E_l(k)T_\omega/\hbar$ of the system (2) for $F = 0$. The parameters are the same as in Fig. 1 and $\hbar = 0.5$. Only the states with mean kinetic energy less than $25\hbar^2$ (a) and less than $35\hbar^2$ (b) are shown.

embedded regions of regular motion. Thus, large stability islands (like those in Fig. 1a) typically survive after applying a moderate dc field.

The quantum analysis of the system (1), (2) is based on the notion of quasi-energy states $\psi_{l,k}(x)$, which by definition are the eigenstates of the system evolution operator $\widehat{U}$ over the period T_ω of the driving frequency ω,

$$\widehat{U}\psi_{l,k}(x) = \exp[-\mathrm{i}E_l(k)T_\omega/\hbar]\psi_{l,k}(x)\,, \tag{4}$$

$$\widehat{U} = \widehat{\exp}\left(-\frac{\mathrm{i}}{\hbar}\int_0^{T_\omega}\widehat{H}(t)\,\mathrm{d}t\right), \quad T_\omega = \frac{2\pi}{\omega}. \tag{5}$$

In the pure oscillatory case, the operator (5) obviously commutes with the translational operator over the lattice period, $\hat{a} = \exp(-2\pi\partial/\partial x)$, and, therefore, the quasi-momentum k is a good quantum number.

Fig. 3 shows the quasi-energy spectrum $\lambda = E_l(k)T_\omega/\hbar$ of the system for the parameters of Fig. 1 and (scaled) Planck constant $\hbar = 0.5$. For the almost regular case $\epsilon = 0.1$ in Fig. 3a, the spectrum is dominated by the three classical nonlinear resonances seen in Fig. 1a. The horizontal bands are associated with the central resonance, while the bands with the slope 2π (forming a rhombus) originate from the primary resonances with $m = \pm 1$ (see Eq. (3)). The presence of the chaotic component separating the primary resonances reflects the system local nonintegrability and manifests itself in clear avoided crossings between "primary resonance bands". The bands looking like straight lines correspond to classically ballistic (almost free) motion. For the chaotic case, $\epsilon = 1.5$, the quasi-energy spectrum is typical for a globally nonintegrable quantum system and contains many avoided crossings. A statistical analysis of the spectrum is an appropriate approach in this case [14,15]. We also note that by closer inspection of the spectrum depicted in Fig. 3b one can also find a sign of resonances with $m = \pm 1$ and $m = \pm 2$, although these resonances are hard to detect in Fig. 1b.

We proceed with the case $F \neq 0$. For the $F \neq 0$ evolution operator (5) generally does not commute with the operator of lattice translation. An exception is the case, where the period of the driving frequency T_ω is commensurable with the so-called Bloch period $T_B = \hbar/F$, i.e., $rT_\omega = qT_B$, r, q are integers [16]. In this paper we mainly consider the case $r = 1$, $q = 1$, where the explicit form of the evolution operator over the common period $T = T_\omega = T_B$ is [11,17]

$$\widehat{U} = \mathrm{e}^{-\mathrm{i}x}\widehat{\exp}\left(-\frac{\mathrm{i}}{\hbar}\int_0^{T}\widetilde{H}(t)\,\mathrm{d}t\right), \tag{6}$$

with

$$\widetilde{H}(t) = (\hat{p} - Ft)^2/2 + \cos[x - \epsilon\sin(\omega t)]\,. \tag{7}$$

Because we are interested in the metastable states, the operator (6) should be diagonalized with the resonance boundary condition, which corresponds to a vanishing probability to find a particle with a positive momentum,

$$\lim_{p\to\infty}|\psi_{l,k}(p)|^2 \to 0\,. \tag{8}$$

In a numerical calculation the condition (8) can be automatically satisfied by truncating the operator $\widehat{U}$ in momentum space [17,18].

In the quasi-regular case (a) the spectrum of the system's metastable states is shown in Fig. 4[4]. The

[4] For the sake of comparison with Fig. 3 the spectrum in Figs. 4–6 is actually presented for $H = p^2/2 + \cos[x - \epsilon\cos(\omega t)] + Fx$ instead of $H = p^2/2 + \cos[x - \epsilon\sin(\omega t)] + Fx$. In the latter case the spectrum is as shown but shifted by 1/4 over k. (A shift of the field phase obviously does not affect the quasi-energy spectrum in Fig. 3.)

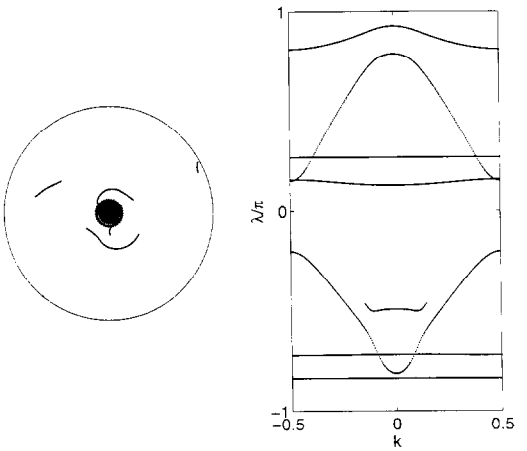

Fig. 4. Complex quasi-energies $E_l(k)$ in the quasi-regular case (a). The circular plot on the left shows the phase $\lambda = \mathrm{Re}[E_l(k)]T/\hbar$ against the decay coefficient $\Gamma = \exp(-\mathrm{Im}[E_l(k)]T/\hbar)$. The plot on the right presents k-dependence of the phase λ, only the states with $\Gamma > \exp(-2)$ are shown.

parameters are the same as in Fig. 3a, and $F \approx 0.13$ is chosen to satisfy the condition $T_\omega = T_B$. The circular diagram on the left depicts the complex quasi-energy spectrum in polar coordinates and the plot on the right presents the k-dependence of the real part of the quasi-energy. It is seen that the complex quasi-energies are arranged in bands, which resembles the nonlinear resonance band structure in Fig. 3a. Thus, we can conclude that the most stable states are those associated with primary nonlinear resonances. This conclusion is in agreement with the classical picture where, as mentioned above, the islands of regular motion survive after applying a static field. We would also like to stress that the crossing of the bands seen in Fig. 4 (and later on in Fig. 5) is an artificial fact due to the two-dimensional presentation of three-dimensional space spanned by the quasi-energies (see Fig. 5).

Fig. 6 shows the spectrum of the metastable states in the chaotic case (b). It is seen that the k-dependence of both real and imaginary parts of the quasi-energies $E_l(k)$ is quite irregular and a statistical approach seems to be an appropriate one to analyze the spectrum. Such a statistical analysis will be the subject of a forthcoming study. Here we only present the distribution of the imaginary parts of the quasi-energies, more precisely, the distribution $f(\tau)$ of decay times of the quantum metastable states

$$\tau = \hbar/2\,\mathrm{Im}[E_l(k)] \qquad (9)$$

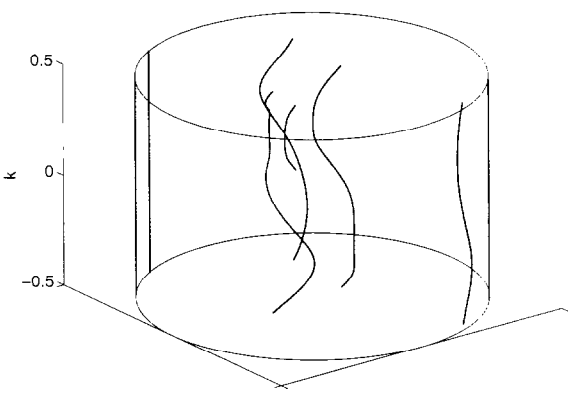

Fig. 5. The same as in Fig. 4 but using 3D presentation for the complex quasi-energies.

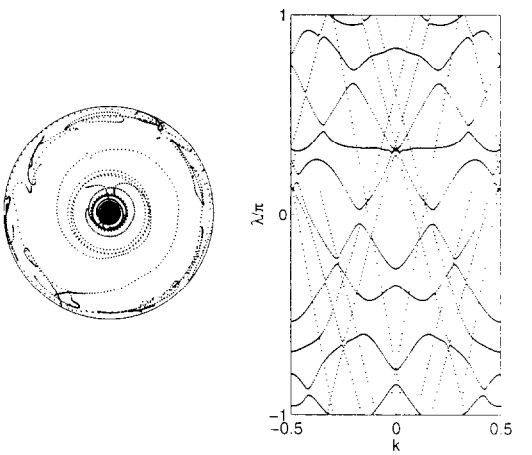

Fig. 6. Complex quasi-energies in the chaotic case (b). The phases in the right-hand plot are shown only for the states with $\Gamma > \exp(-1)$.

in Fig. 7. A remarkable feature of the distribution shown is the existence of states with an extremely large decay time τ in comparison to the classical decay time $\tau_{\mathrm{cl}} \approx 10T$. (The numerical data suggests asymptotic $f(\tau) \sim \tau^{-2}$ for $\tau \gg T$.) Thus the quantum system is essentially more stable against a static field than the classical one. This statement is confirmed by direct numerical simulation of wave packet dynamics. The solid line in Fig. 2 shows the probability of a quantum wave packet to "stay within the chaotic region"

$$P_{\mathrm{qu}}(t) = \int_{|p|<6} |\psi(p,t)|^2\,\mathrm{d}p\,.$$

Here the initial wave function was chosen as a min-

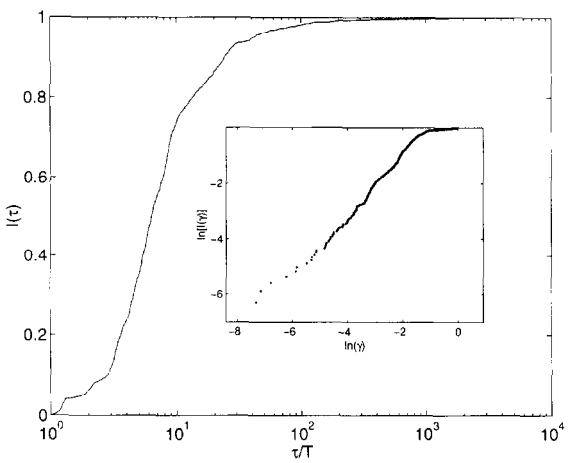

Fig. 7. Integrated distribution function $I(\tau) = \int_T^\tau f(\tau')\,d\tau'$ of quantum decay times $\tau = \hbar/2\,\mathrm{Im}[E_l(k)]$ in the chaotic case (b). Note that the τ-axis is in logarithmic scale. The insert shows the integrated distribution for $\gamma = T/\tau$.

imal uncertainty Gaussian packet centered at $x = 0$, $p = 0$. A clear deviation from the classical behavior is noticed. For the moment we have no explanation for this quantum stabilization phenomenon. However, it can be stated for sure that this quantum stabilization is a consequence of the resonance condition between the period of the driving frequency and the Bloch period. The dashed line in Fig. 1 shows the function $P_{\mathrm{qu}}(t)$ for the *same* values of ω, ϵ and F, however, for $\hbar = 0.5109531$ instead of $\hbar = 0.5$. It is seen that in this case the quantum behavior seems to follow the classical one. We also would like to stress that the quantum stabilization discussed is not a particular feature of the system (1). The same phenomenon was noticed earlier for a different chaotic system with the Hamiltonian $H = p^2/2 + \cos(\omega t)\cos x + Fx$ [11].

We believe it is useful to compare our approach with that based on the tight-binding model in some more detail. For the problem considered the tight-binding Hamiltonian has the form

$$\hat{H} = -\frac{\Delta}{4}\sum_l (|l+1\rangle\langle l| + |l\rangle\langle l+1|) + [F + F_\omega \sin(\omega t)]\sum_l 2\pi l|l\rangle\langle l|, \qquad (10)$$

where l labels the lattice cites and Δ is the width of a single Bloch band. The advantage of this model (10) is that (provided the resonance condition is satisfied) it can be solved analytically [7–10]. However, if we wish to relate the problem (10) to the general system (1), a condition justifying that interband transitions may be neglected should be met. It is easy to see that this is *not* the case for the system parameters presently used. In fact, as has already been seen in Fig. 3, the system is in a regime of strong band coupling induced by the periodic field (every avoided crossing can be identified with a particular multiphoton transition). Thus, the regimes of the system dynamics discussed in this paper *cannot* be studied by using a tight-binding model in principle.

To summarize, we have numerically analyzed the metastable states of a Bloch particle in the presence of ac and dc fields for a resonance between the Bloch period and the period of an ac field. For a small amplitude of the driving field a perturbative approach can be used and the complex spectrum of the quasi-energies has a regular structure. In contrast, for a large amplitude the spectrum should be regarded as chaotic (quasi-random). The statistical analysis of the spectrum shows the presence of an algebraic tail for the distribution of the resonance widths (imaginary part of the quasi-energy), which is responsible for the phenomenon of quantum stabilization. We believe that this new phenomenon can be well observed in experiments with cold atoms in an optical lattice [5,19,20]. (It is an appropriate place here to note that the dimensionless values of the driving frequency ω and the amplitude ϵ used in our numerical calculation correspond to the scaled frequency and amplitude of laser field modulation used in the experiment [5].) Since a small value of the scaled Planck constant requires a pretty large intensity of the laser field, special efforts to decrease the effect of spontaneous emission (which causes an incoherent scattering of the atoms similar to scattering of electrons by impurities in a solid crystal) should be taken[5] Fortunately, recent progress in

[5] For the system "an atom in a standing laser wave" the scaled Planck constant is given by $\hbar' = 4(2\hbar k^2\delta/m\Omega_{\mathrm{R}}^2)^{1/2}$, where Ω_{R} is the Rabi frequency, δ the detuning, m the atomic mass, and k the wave vector of a standing wave (for this scaling see, for example, Ref. [21]). Thus the scaled Planck constant is inversely proportional to the intensity of the laser field. The effect of spontaneous emission is characterized by the atomic diffusion constant $D = \hbar^2 k^2 \Gamma \Omega_{\mathrm{R}}^2/2\delta^2$, where Γ is the natural width of the optical transition. It is seen from the last formula that the effect of spontaneous emission can be suppressed only for large detuning.

the experimental techniques indicates that the effect of spontaneous emission can be very well controlled in the experiment with cold atoms [19,20].

References

[1] M. Raizen, C. Solomon, Qian Niu, Physics Today, July 1997, 30.
[2] J.E. Avron, Ann. Phys. (NY) 143 (1982) 33.
[3] G. Nenciu, Rev. Mod. Phys. 63 (1991) 91.
[4] R. Graham, M. Schlautmann, D.L. Shepelyansky, Phys. Rev. Lett. 67 (1991) 2.
[5] J.C. Robinson, C. Bharucha, F.L. Moore, R. Jahnke, G.A. Georgakis, Q. Niu, M.G. Raizen, B. Sundaram, Phys. Rev. Lett. 74 (1995) 3963.
[6] F.H. Faisal, J.Z. Kamiński, Phys. Rev. A 54 (1996) R1769.
[7] D.H. Dunlap, V.M. Kenkre, Phys. Rev. B 34 (1986) 3625.
[8] Nguyen Hong Shon, H.N. Nazareno, J. Phys. Condens Matter 4 (1992) L611.
[9] X.-G. Zhao, R. Jahnke, Q. Niu, Phys. Lett. A 202 (1995) 297.
[10] M. Holthaus, G.H. Ristow, D.W. Hone, Europhys. Lett. 32 (1995) 241.
[11] M. Glück, A.R. Kolovsky, H.-J. Korsch, Phys. Rev. E, in press.
[12] A.J. Lichtenberg, M.A. Lieberman, Regular and Chaotic Dynamics (Springer, Berlin, 1983).
[13] P.J. Bardroff, I. Bialynicki-Birula, D.S. Krämer, G. Kurizki, E. Mayr, P. Stifter, W.P. Schleich, Phys. Rev. Lett. 74 (1995) 3959.
[14] S. Miayzaki, A.R. Kolovsky, Phys. Rev. E 50 (1994) 910.
[15] A.R. Kolovsky, Phys. Rev. E 56 (1997) 2261.
[16] J. Zak, Phys. Rev. Lett. 71 (1993) 2623.
[17] M. Glück, A.R. Kolovsky, H.-J. Korsch, N. Moiseyev, EPJ (part D), in press.
[18] M. Glück, A.R. Kolovsky, H.-J. Korsch, A truncated shift-operator technique for the calculation of resonances in Stark systems, preprint (1998).
[19] B.G. Klappauf, W.H. Oskay, D.A. Steck, M.G. Raizen, to appear in Phys. Rev. Lett.
[20] H. Ammann, R. Gray, N. Christensen, I. Shvarchuck, J. Phys. B 31 (1998) 2449.
[21] A.R. Kolovsky, H.J. Korsch, Phys. Rev. A 55 (1997) 4433.